Dyes and Pigments 80 (2009) 271–278

Contents lists available at ScienceDirect

Dyes and Pigments

journal homepage: www.elsevier.com/locate/dyepig

Interaction of bovine serum albumin with Acridine Orange (C.I. Basic Orange 14) and its sonodynamic damage under ultrasonic irradiation

Jun Wang [a,b,*], Yuan-Yuan Zhang [a], Ying Guo [b], Lei Zhang [a], Rui Xu [a], Zhi-Qiang Xing [a], Shi-Xian Wang [a], Xiang-Dong Zhang [a]

[a] Department of Chemistry, Liaoning University, Shenyang 110036, PR China
[b] Department of Pharmacy, Liaoning University, Shenyang 110036, PR China

ARTICLE INFO

Article history:
Received 24 April 2008
Received in revised form 24 July 2008
Accepted 30 July 2008
Available online 20 August 2008

Keywords:
Bovine serum albumin
Acridine orange dye
Interaction
Sonodynamics
Damage
Ultrasonic irradiation

ABSTRACT

The interaction of acridine orange (C.I. Basic Orange 14) with bovine serum albumin and the subsequent sonodynamic damage to bovine serum albumin imparted by ultrasonic irradiation were studied. The quenching constant, binding constant and the binding site number were measured using fluorescence quenching. The distance of binding between the dye and the serum albumin was obtained according to Föster's nonradiative energy transfer theory. The effects of ultrasonic irradiation time, dye concentration, pH and ionic strength on bovine serum albumin were determined using UV–vis and fluorescence spectra; the extent of damage was enhanced by a increases in irradiation time, dye concentration and ionic strength, but was reduced by an increase in pH.

1. Introduction

Acridine orange (C.I. Basic Orange 14; AO) is a heterocyclic compound (Fig. 1) that enjoys usage in printing, dyeing, leather, printing inks and lithography [1]. In histochemistry, the dye is extensively used for biological staining to differentiate DNA from RNA by fluorescence emission [2]. Moreover, due to its planar structure, AO dye has been selected as a probe to investigate the small molecule interactions with DNA [3,4]. More importantly, AO dye has been used as a kind of photosensitive drug showing promising applications for anticancer treatment and tumor diagnoses [5–7].

Serum albumin, as one of the most abundant carrier proteins, plays an important role in the transport and disposition of endogenous and exogenous ligands present in blood. Distribution and metabolism of many biologically active compounds such as metabolites, drugs and other organic compounds in the body are correlated with their affinities towards serum albumin [8,9]. Consequently, the bovine serum albumin (BSA) is selected as a drug targeting to study the interaction and oxidative damage effect because of its low cost, ready availability and the results of all the studies are consistent with the fact that BSA and human serum albumins (HSAs) are homologous proteins [10,11].

The method of diagnosing and treating tumors using a photosensitiser was termed photodynamic treatment (PDT) by Doughtery and his workgroup in 1978 [12–15]. PDT is based on selective accumulation of photosensitiser in transformed tissue and irradiation light with appropriate wavelength. During treatment, the photosensitiser can be activated by ultraviolet or visible light and transferred into an excited triplet state. The excited states can undergo rapid and efficient energy transfer to triplet oxygen ($^3O_2$) to give singlet oxygen ($^1O_2$), which will oxidize a wide range of biological targets including DNA, RNA, proteins, lipids, and sterols [16–18]. However, PDT is mainly used to cure shallow tumors such as skin cancer and lung cancer, because of the short penetration distance of ultraviolet and visible light [19]. Contrary, ultrasound has exceedingly strong penetrating ability and mature focusing technology, so the researchers have paid great attention to the use of ultrasonic irradiation instead of light to activate photosensitisers. In 1989, at the International Conference, Umemura et al., submitted their research on killing cancerous cells and suppressing the tumor growth by activating some photosensitive dyes as sonosensitisers upon ultrasonic irradiation. And they called this method as sonodynamic treatment (SDT) [20–22]. The sonosensitisers themselves generally have no antitumor effect, but after being activated by

* Corresponding author. Department of Chemistry, Liaoning University, Shenyang 110036, PR China. Tel.: +86 024 81917150; fax: +86 024 62202053.
E-mail addresses: wangjun890@126.com, wangjun888@vip.sina.com (J. Wang).

0143-7208/$ – see front matter © 2008 Elsevier Ltd. All rights reserved.
doi:10.1016/j.dyepig.2008.07.013

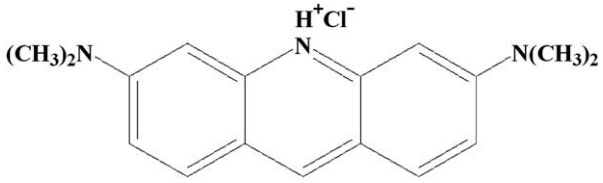

Fig. 1. Molecular structure of Acridine Orange (AO).

ultrasound, they display strong antitumor activity. Considering the selectivity of many sonosensitisers to tumor tissue, therefore, the SDT has wide application prospect in aspect of tumor treatment.

Over the past few years much research has been undertaken on ultrasound apparatus, experimental conditions, therapeutic effect on tumors and reaction mechanism of SDT. But, all of them regarded the tumor cells as target, and achieved the goal of treating tumors through damaging the cell membrane resulting in cell death [23,24]. In fact, the differences of membranes between natural and tumor cells are quite little. Therefore, in order to research and develop the target drug and improve the selectivity of SDT, researchers should consider some biological macromolecules as molecular targeting. If some biological macromolecules such as DNA, RNA, protein and enzyme in cells are damaged, these cells will die in a short time. So in this work, we selected BSA as a molecular target and AO as a sonosensitiser. Since the $^1O_2$ which is produced by sonosensitiser has very short lifetime, it only can diffuse 20 nm [25], the interaction or close proximity between sonosensitiser and target molecules for sonodynamic damage is necessary. The interaction of AO dye molecule to BSA was reported [26], but it was not complete and detailed. Therefore, in this paper, we divided the experiment into two steps. Firstly, the quenching of intrinsic fluorescence was used as a tool to study the interaction of AO dye to BSA in an attempt to calculate the quenching constant (K_{sv}), the binding site number (n), the apparent binding constant (K_A) and the binding distance (r), respectively. Secondly we studied the damage of BSA molecules in the presence of AO dye under ultrasonic irradiation. In addition, some influencing factors such as ultrasonic irradiation time, AO dye concentration, solution acidity and ionic strength on the damage of BSA molecules were also studied systemically.

2. Experimental section

2.1. Materials

Commercially prepared bovine serum albumin (BSA, purity >99.0%) was obtained from Beijing Abxing Biological Technology Company and stored at 4.0 °C in refrigerator. Acridine orange dye (AO dye, purity >99.0%) was purchased from Sigma Chemistry Company. Tris-HCl–NaCl buffer solution (50 mmol/L Tris-HCl, 50 mmol/L NaCl and pH = 7.4) was prepared by dissolving 50 mmol Tris and 50 mmol NaCl in 800 mL double distilled water, and then adjusting the pH value to 7.4 using 0.25 mol/L HCl solution. The mixed solution was diluted to 1000 mL with double distilled water. All the chemicals were of analytical reagent grade, and double distilled water was used for all solution preparation.

2.2. Apparatus and instruments

The Controllable Serial-Ultrasonics apparatus (SG3200HE, Shanghai GuTel Ultrasonic Instrument Company, LTD, China) shown in Fig. 2 was used as irradiation source. Its frequency and power were 59 kHz and 165 W, respectively. The fluorescence measurements were performed on a fluorophotometer (Cary 300, Varian Company, USA) and the UV–vis spectra were recorded with

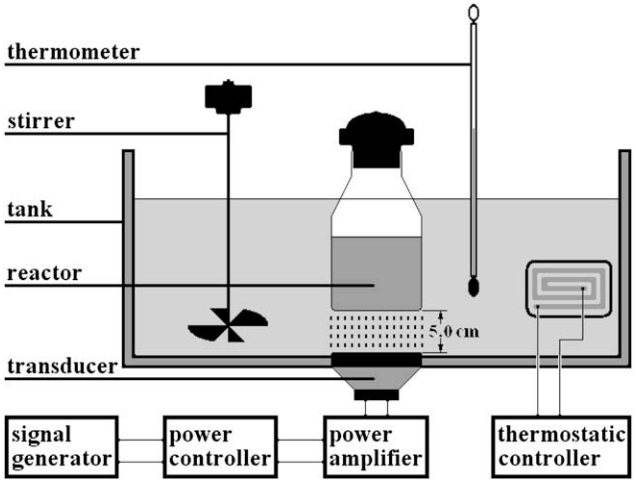

Fig. 2. The apparatus of ultrasonic irradiation.

an UV–vis spectrophotometer (Cary 50, Varian Company, USA). The pH value of solutions was measured with a pH meter (PHS-3C, Shanghai Leici Instrument Company, LTD, China).

2.3. Measurement of binding parameters

The BSA and AO stored solutions were prepared in Tris-HCl–NaCl buffer solution (50 mmol/L Tris-HCl, 50 mmol/L NaCl and pH = 7.4). The concentrations of the BSA and AO stored solutions were 2.0×10^{-5} mol/L and 5.0×10^{-5} mol/L, respectively. To a 25.00 mL volumetric flask, the 12.50 mL BSA solution with 2.0×10^{-5} mol/L and appropriate volume of AO solution with 5.0×10^{-5} mol/L were added in order. The volume of mixture solutions was diluted to 25.00 mL with Tris-HCl–NaCl buffer solution. The final concentration of BSA was 1.0×10^{-5} mol/L. The concentrations of AO dye were varied from 0 to 2.5×10^{-5} mol/L at 0.5×10^{-5} mol/L interval. The other conditions such as solution acidity of pH = 7.4, NaCl concentration of 50 mmol/L, temperature of 37.00 ± 0.02 °C and total volume of 25.00 mL were adopted. The fluorescence spectra were recorded in the wavelength of 250–550 nm upon excitation at 280 nm and 5.0 nm/5.0 nm slit widths. All test solutions were incubated for 10 min before measurement. The curves of fluorescence quenching spectra are shown in Fig. 3. The maxima intensity values in the fluorescence spectra were recorded for the next calculation of quenching parameters. The related plots of quenching equation are shown in Figs. 4 and 5. In order to calculate the binding distance, the spectral overlap of BSA fluorescence and AO absorption is shown in Fig. 6.

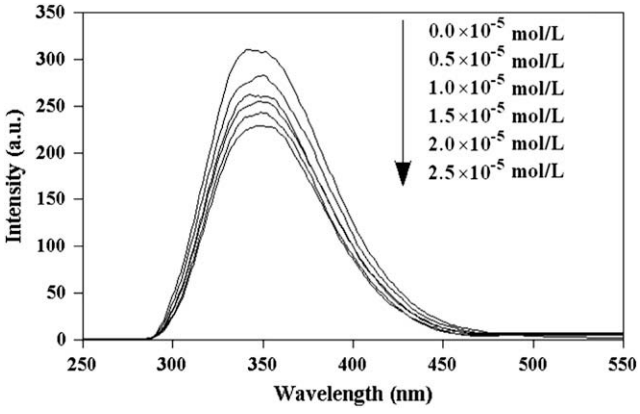

Fig. 3. Fluorescence spectra of BSA solutions (1.0×10^{-5} mol/L) with the increase of AO dye concentration.

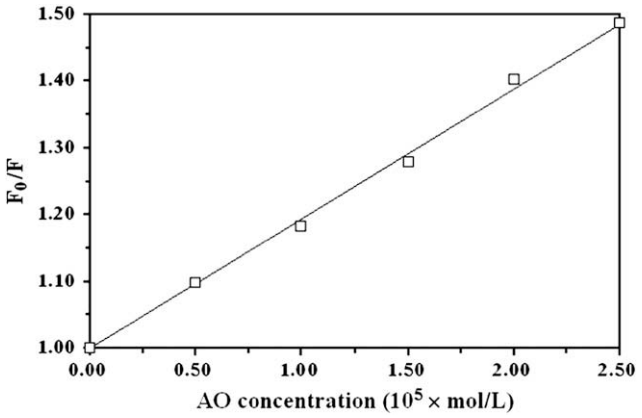

Fig. 4. Stern–Volmer plot of BSA solution (1.0×10^{-5} mol/L) with the increase of AO dye concentration.

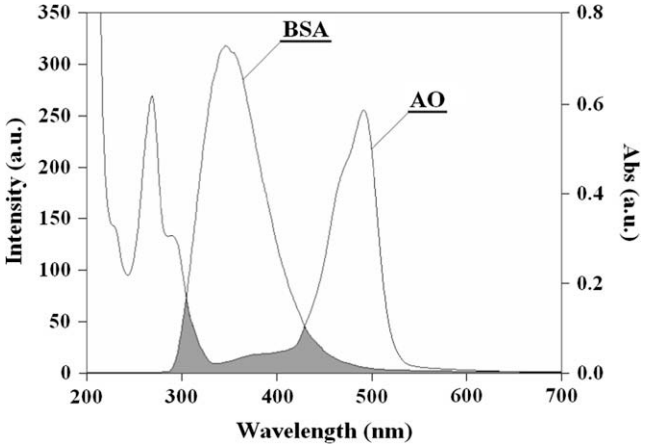

Fig. 6. Spectral overlap of BSA fluorescence ($\lambda_{ex} = 280$ nm) and AO absorption ([BSA] = [AO] = 1.0×10^{-5} mol/L).

2.4. Measurement of damage procedure

Firstly, six clean 25.00 mL volumetric flasks were marked as **a**–**f**, respectively. Four 12.5 mL BSA stored solutions with concentration of 2.0×10^{-5} mol/L were took exactly and put into volumetric flasks **a**–**d**, respectively. And then four 5.00 mL AO stored solutions with concentration of 5.0×10^{-5} mol/L were added to volumetric flasks **a**, **b**, **e** and **f**, respectively. Finally, all of the volumetric flasks were diluted to 25.00 mL with the Tris-HCl–NaCl solution. Afterwards, the solutions were transferred into six conical flasks. Then the conical flasks **a**, **c** and **e** were placed in an ultrasonic irradiation apparatus. The conical flasks **b**, **d** and **f** were kept in dark. After 3.0 h irradiation, the UV–vis and fluorescence spectra of each sample were determined, in order to evaluate the damage degrees to BSA molecules. The results are shown in Figs. 7 and 8, respectively. In order to investigate the ultrasonic damage process systematically, the effects of ultrasonic irradiation time, AO concentration, ionic strength and pH value were reviewed by the UV–vis and fluorescence spectra and the corresponding results are shown in Figs. 9–12, respectively.

3. Results and discussion

3.1. Interaction of AO dye to BSA

From the data in Fig. 3 it is apparent that the fluorescence intensity is quenched along with the increase of AO dye concentration which indicates that there is an interaction of AO with BSA.

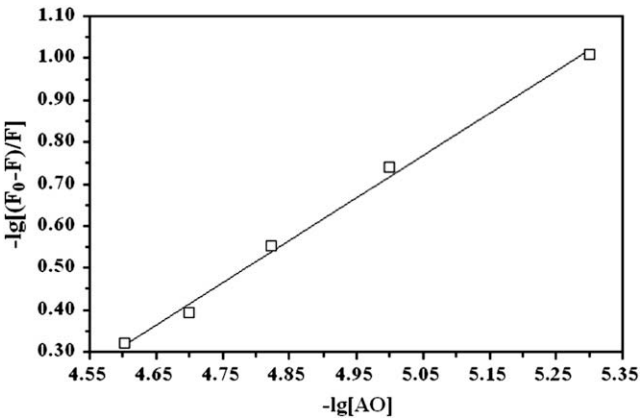

Fig. 5. $\lg(F_0 - F)/F \sim \lg[AO]$ plot of BSA solution (1.0×10^{-5} mol/L).

The data of fluorescence intensities at 348 nm (using excitation wavelength at 280 nm) were analyzed by using Stern–Volmer Eq. (1) [27].

$$F_0/F = 1 + K_q\tau_0[AO] = 1 + K_{SV}[AO] \quad (1)$$

where, F_0 and F are the fluorescence intensities of BSA solutions at 348 nm in the absence and presence of quencher (AO dye), respectively. K_q is the bimolecular quenching constant, τ_0 is the lifetime of the fluorophore and K_{SV} is the Stern–Volmer fluorescence quenching constant. [AO] is the concentration of the quencher, AO.

Fig. 4 displays the Stern–Volmer plots of BSA solution with various AO dye concentrations. The obtained plots exhibit a good linear relationship ($R^2 = 0.998$). From the Stern–Volmer equation, it is known that the K_{SV} is 1.94×10^4 L/mol. For some protein molecules like BSA the τ_0 is known to be approximately 10^{-8} s, thus the K_q is about 1.94×10^{12} L/mol s. Since the maximum value of K_q for the diffusion controlled quenching process of biological macromolecules is about 10^{10} L/mol s, the obtained K_q is much higher than this value. Hence, the dominating quenching mechanism is not dynamic but static. It suggests that the quenching of fluorescence is caused by a specific interaction between BSA molecule and AO dye. It can be considered that the BSA and AO dye form complexes.

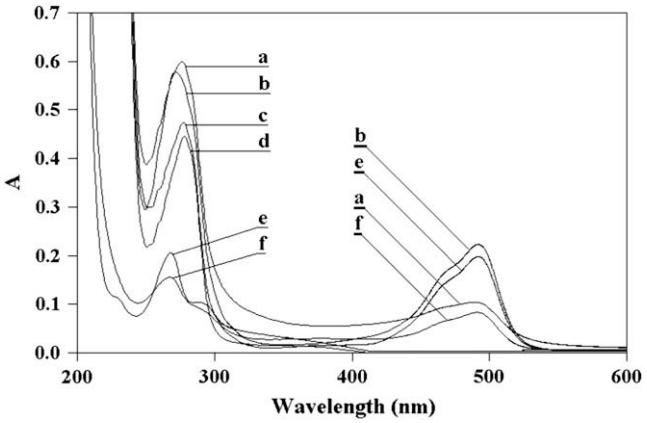

Fig. 7. UV–vis spectra of BSA–AO, BSA and AO solutions at different conditions. a: BSA–AO (with irradiation for 3.0 h); b: BSA–AO (without irradiation); c: BSA (with irradiation for 3.0 h); d: BSA (without irradiation); e: AO (without irradiation); f: AO (with irradiation for 3.0 h).

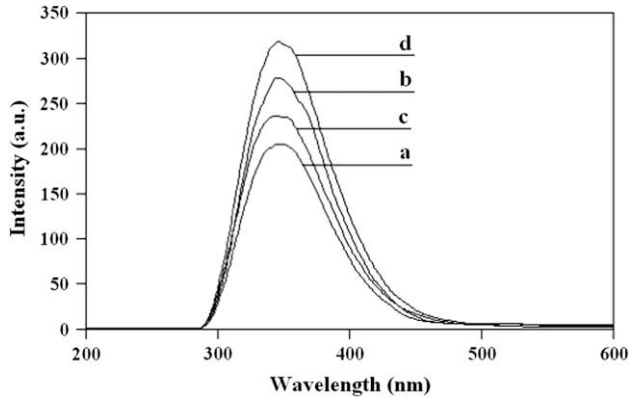

Fig. 8. Fluorescence spectra ($\lambda_{ex} = 280$ nm) of BSA–AO and BSA solutions at different conditions. a: BSA–AO (with irradiation for 3.0 h); b: BSA–AO (without irradiation); c: BSA (with irradiation for 3.0 h); d: BSA (without irradiation).

These data of fluorescence intensities were also used to obtain the binding constant (K_A) and the binding site number (n) by using Eq. (2).

$$\lg(F_0 - F)/F = \lg K_A + n\lg[\mathrm{AO}] \quad (2)$$

K_A and n could be measured from the intercept and slope by plotting $\lg(F_0-F)/F$ against $\lg[AO]$. The linearity of the curves was also rather good ($R^2 = 0.998$).

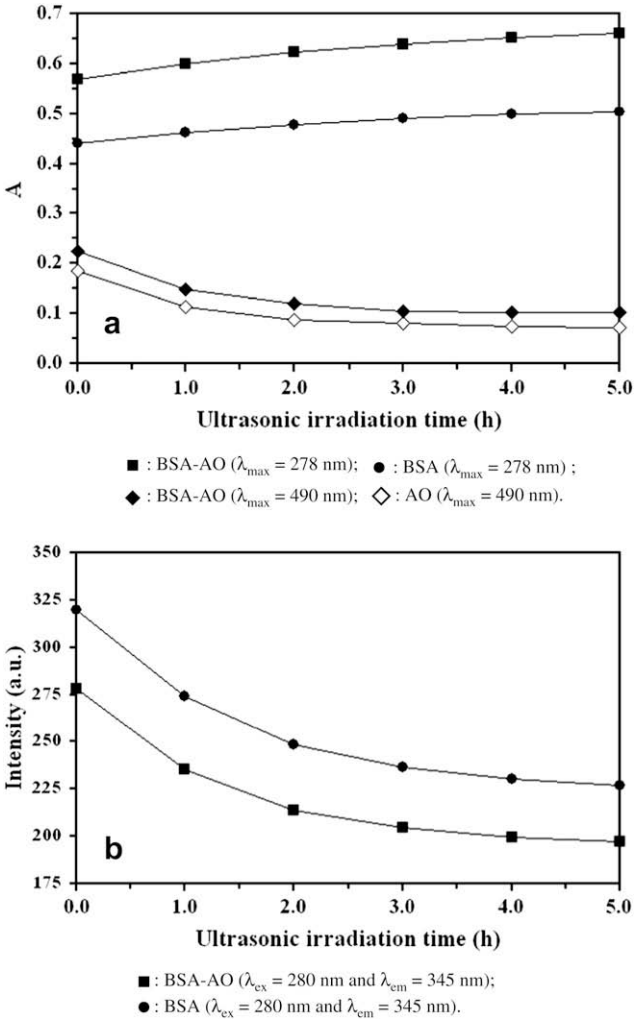

Fig. 9. Changes of absorbances (a) and fluorescence intensities (b) of BSA–AO and BSA solutions with ultrasonic irradiation time. ■: BSA–AO ($\lambda_{max} = 278$ nm); ■: BSA–AO ($\lambda_{ex} = 280$ nm and $\lambda_{em} = 345$ nm); ●: BSA ($\lambda_{max} = 278$ nm); ●: BSA ($\lambda_{ex} = 280$ nm and $\lambda_{em} = 345$ nm). ◆: BSA–AO ($\lambda_{max} = 490$ nm); ◇: AO ($\lambda_{max} = 490$ nm).

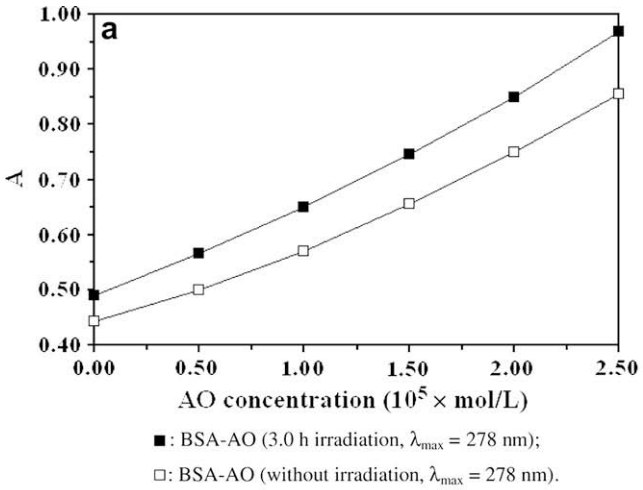

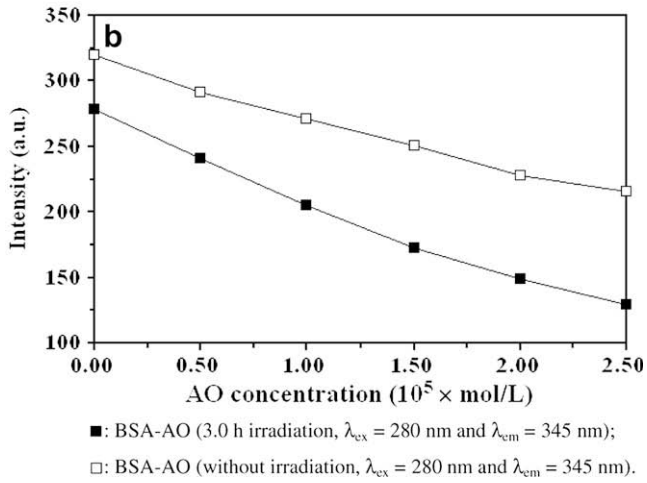

Fig. 10. Changes of absorbances (a) and fluorescence intensities (b) of BSA–AO solutions with AO dye concentration. ■: BSA–AO (3.0 h irradiation, $\lambda_{max} = 278$ nm); ■: BSA–AO (3.0 h irradiation, $\lambda_{ex} = 280$ nm and $\lambda_{em} = 345$ nm); □: BSA–AO (without irradiation, $\lambda_{max} = 278$ nm). □: BSA–AO (without irradiation, $\lambda_{ex} = 280$ nm and $\lambda_{em} = 345$ nm).

According to Fig. 5, K_A and n can be obtained and are 2.01×10^4 L/mol and 1.00, respectively. The comparatively large K_A value indicates that there is a strong interaction between BSA molecule and AO dye. AO dye has a planar structure, and there is less steric hindrance in the binding process. As a result, the binding of AO dye to BSA molecule becomes easier [28]. The n value is equal to 1, indicating that there is one class of binding site for AO dye to BSA molecule [29]. Because of the amphipathic structure of AO dye molecule, the binding force between BSA molecules and AO dye is mainly electrostatic and hydrophobic interactions [30].

Utilizing the K_A value, the free energy change (ΔG_0) value could be calculated from the relationship.

$$\Delta G_0 = -\mathrm{RT}\ln K_A$$

Thus, ΔG_0 is -25.54 kJ/mol for $R = 8.314$ J/mol K and $T = 310$ K. The negative sign for ΔG_0 indicates the spontaneity of the binding of AO dye to BSA molecule.

The distance between BSA and AO dye molecules can be determined according to Föster's nonradiative energy transfer theory [31]. According to this theory, the efficiency (E) of energy transfer between the donor (BSA) and acceptor (AO dye) can be calculated using Eq. (3).

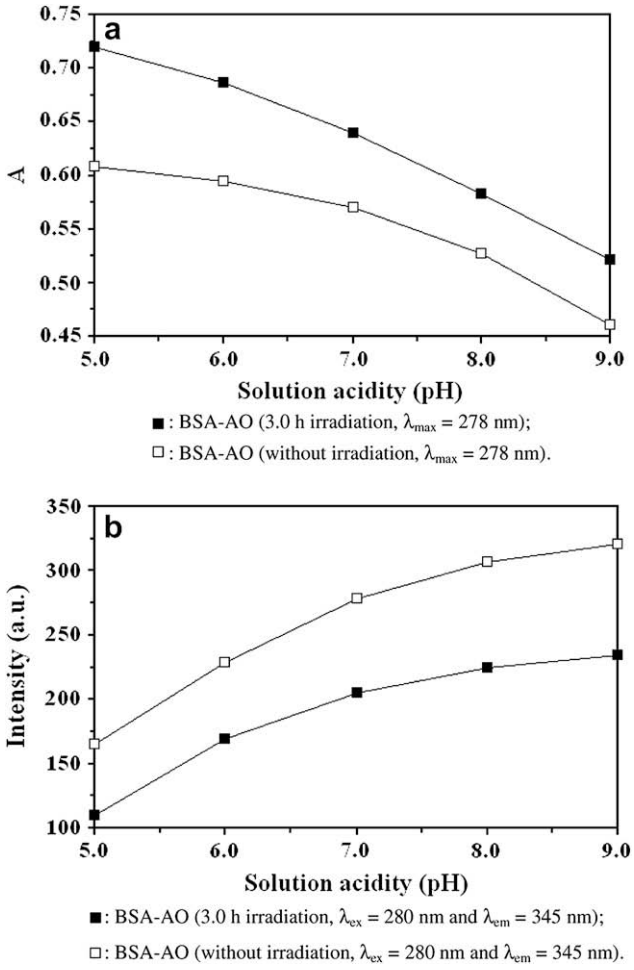

Fig. 11. Change of absorbances (a) and fluorescence intensities (b) of BSA–AO solutions with solution acidity. ■: BSA–AO (3.0 h irradiation, $\lambda_{max} = 278$ nm); ■: BSA–AO (3.0 h irradiation, $\lambda_{ex} = 280$ nm and $\lambda_{em} = 345$ nm); □: BSA–AO (without irradiation, $\lambda_{max} = 278$ nm). □: BSA–AO (without irradiation, $\lambda_{ex} = 280$ nm and $\lambda_{em} = 345$ nm).

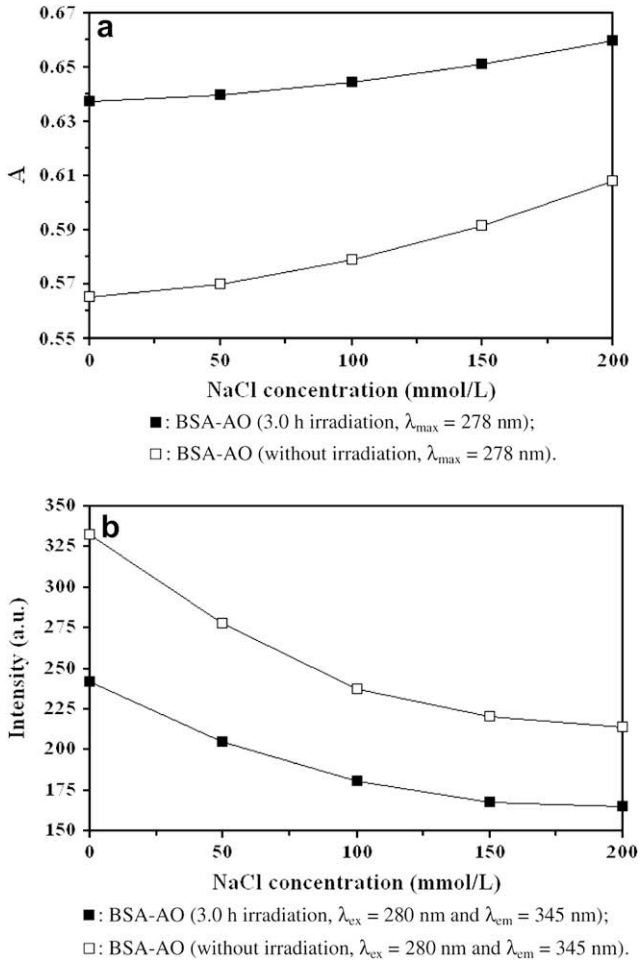

Fig. 12. Change of absorbances (a) and fluorescence intensities (b) of BSA–AO solutions with NaCl concentration. ■: BSA–AO (3.0 h irradiation, $\lambda_{max} = 278$ nm); ■: BSA–AO (3.0 h irradiation, $\lambda_{ex} = 280$ nm and $\lambda_{em} = 345$ nm); □: BSA–AO (without irradiation, $\lambda_{max} = 278$ nm). □: BSA–AO (without irradiation, $\lambda_{ex} = 280$ nm and $\lambda_{em} = 345$ nm).

$$E = 1/\left[1 + (r/R_0)^6\right] \tag{3}$$

where r is the binding distance between the donor and acceptor, and the R_0 is the critical binding distance when the transfer efficiency (E) is 50%, which can be calculated by Eq. (4).

$$R_0^6 = 8.8 \times 10^{-25}\left(K^2 n^{-4} \varphi \mathrm{D}^{\mathrm{J}}\right) \tag{4}$$

where K^2 is the spatial orientation factor of the dipole, here the n is the refractive index of medium, the φ_D is the quantum yield of the donor in the absence of acceptor and the J is the overlap integral of the fluorescence emission spectrum of the donor and the absorption spectrum of the acceptor. In the present case, K_2, n and φ_D are 2/3, 1.336 and 0.15 for BSA, respectively. And then, the J can be obtained by Eq. (5).

$$J = \sum F(\lambda)\varepsilon(\lambda)\lambda^4 \Delta\lambda / \sum F(\lambda)\Delta\lambda \tag{5}$$

where λ is the wavelength of corresponding fluorescence intensity of BSA and absorbance of AO dye. $F(\lambda)$ and $\varepsilon(\lambda)$ are the fluorescence intensity of BSA and the absorbance of AO dye at λ, respectively.

Fig. 6 shows the overlap of fluorescence emission spectrum of BSA and ultraviolet absorption spectrum of AO dye. The efficiency (E) of energy transfer can be determined by Eq. (6).

$$E = 1 - F/F_0 \tag{6}$$

According to the above Eqs. (3)–(6), J, R_0, E and r were calculated, that is, $J = 5.60 \times 10^{-15}$ cm^3 L/mol, $R_0 = 2.32$ nm, $E = 0.124$ and $r = 3.21$ nm. Obviously, the acceptor–donor distance is less than 7.0 nm, which indicates that the energy transfer from BSA to AO dye occurs with high possibility. Therefore, it indicates that the binding of AO dye to BSA is through energy transfer, which quenched the fluorescence of BSA [32]. It is well known that the exposure of AO dye to ultrasonic irradiation can generate a large amount of $^1O_2$ [33]. The result of the short distance between BSA and AO dye means that the $^1O_2$ has a greater opportunity to attack the BSA molecules even though its lifetime is short. Therefore, the damage of BSA molecules in the presence of AO dye under ultrasonic irradiation is feasible in theory.

3.2. UV–vis and fluorescence spectra of BSA–AO solutions under ultrasonic irradiation

From Fig. 7 it can be seen that the pure BSA solution has only one strong absorption peak (curve d) at 278 nm, while the pure AO dye solution has two absorption peaks (curve e) at 260 nm and 490 nm respectively. When the BSA and AO dye solutions are mixed ($[BSA] = [AO] = 1.0 \times 10^{-5}$ mol/L), the remarkable hyperchromic effect and slight blue shifts (from 278 nm to 272 nm) are both observed (curve b). It indicates that the changes in the conformation of BSA occur, the peptide strand extends, and the hydrophobicity

increases [34]. The major chromophoric amino acids of BSA molecules are tryptophan (Trp), tyrosine (Tyr), phenylalanine (Phe), etc. Hence, the interaction of AO dye to BSA causes the increase and slight blue shift of absorption peak.

Then, all of the above-mentioned solutions were irradiated by ultrasound for 3.0 h. Both of the BSA solution (curve c) and the BSA–AO solution (curve a) showed hyperchromic effect at 278 nm compared with corresponding ones (curves d and b) without irradiation. However, the BSA–AO solution exhibited more obvious hyperchromic effect. It can be explained that AO dye can be easily activated and undergo efficient energy transfer to $^3O_2$ to give $^1O_2$. These $^1O_2$ will attack the BSA molecules in a short time, which caused the extension of the peptide strand, the decrease of hydrophobicity and the destruction of BSA spatial structure. Hence, the chromophoric amino residues are further exposed. The degree of damage to the BSA in BSA–AO solution is more obvious compared with the pure BSA solution. In addition, in the absorption curves of pure AO solution (curve f) and the BSA–AO (curve a) solution the absorption peaks at 490 nm decrease compared with those without ultrasonic irradiation. It can be concluded that under ultrasonic irradiation the AO dye, which is a good generator of $^1O_2$, not only can damage the BSA molecules but also degrade itself at the same time. Therefore, after ultrasound treatment, the AO dye residue in the human body should be little, and the patients do not need to avoid light for a long time, which decreases the skin phototoxicity and side effect to human body.

The foregoing inferences can be further validated by means of fluorescence spectroscopy. As shown in Fig. 8, without ultrasonic irradiation, after adding AO dye to BSA solution, the fluorescence intensity of BSA–AO solution (curve b) was quenched compared with the pure BSA solution (curve d). Of course, it is due to the interaction of AO dye to BSA. With ultrasonic irradiation, there was a fast decrease in fluorescence intensity of both BSA–AO solution (curve a) and BSA solution (curve c). However, the loss of fluorescence intensity of BSA–AO solution was more serious compared with that of pure BSA solution. Therefore, the BSA–AO solution under ultrasonic irradiation emitted the weakest fluorescence in all of the samples. These phenomena can be explained as follows. The intrinsic fluorescence from BSA molecules is mainly due to the excitation of Trp and Tyr residues although their amounts are relatively low (two Trp and 19 Tyr). Under ultrasonic irradiation, the more serious damage of BSA molecules in BSA–AO solution takes place. That is, the number of Trp and Tyr residues gradually decreases [35,36], which is due to the oxidative damage. These results are accordant with those from UV–vis method mentioned above.

3.3. Effect of ultrasonic irradiation time on damage of BSA

The damage of BSA in the presence of AO dye as sonosensitiser was studied along with ultrasonic irradiation time. The concentrations of BSA and AO dye were both 1.0×10^{-5} mol/L. The ultrasonic irradiation time was altered within 5.0 h at 1.0 h interval.

Fig. 9(a) shows the change of the absorbance of BSA solutions at 278 nm under ultrasonic irradiation in the presence and absence of AO dye. It can be seen that the absorbance increase along with the increase of ultrasonic irradiation time both in the presence and absence of AO dye. Moreover, the absorbance of BSA–AO mixed solutions is much higher than corresponding ones of pure BSA solution. That is, the hyperchromic effects of BSA–AO mixed solutions are more obvious than those of the pure BSA solutions at any irradiation time. Otherwise, the absorbance of AO at 490 nm decreases with the increase of ultrasonic irradiation time obviously. It demonstrates that the activated AO dye can not only damage the BSA molecules but also degrade itself at the same time. Fluorescence spectra were also used to study the effect of ultrasonic irradiation time on the damage of BSA. The corresponding results are shown in Fig. 9(b). It can be seen that the fluorescence intensities decrease along with the increase of ultrasonic irradiation time. In this case, the loss of intrinsic fluorescence of BSA is mainly due to the oxidation of its Trp and Tyr residues. Nevertheless, the fluorescence intensities of BSA–AO solution are obviously lower than those of BSA solution at any irradiation time which indicates that the damage of BSA is more likely to happen in the BSA–AO solution because of the synergistic effect of ultrasound and AO dye.

It can be inferred that the BSA molecules both in the presence and absence of AO dye suffer from different degrees of damage under ultrasonic irradiation. The damage of BSA molecules in BSA–AO solution is more serious compared with that in the pure BSA solution. Moreover, the degree of damage of BSA is enhanced with increasing ultrasonic irradiation time. These results can be explained as follows. Activating sonosensitive dye AO can generate a large flux of $^1O_2$. Therefore, the damage degrees are improved in a large scale. Meanwhile, along with the increase of ultrasonic irradiation time, the quantity of $^1O_2$ generated in the solutions also increases, and the chance that $^1O_2$ attacks BSA molecules becomes greater. Therefore, the damage of BSA becomes more serious. It is also apparent that the anticipated level of protein damage can be achieved through appropriate adjustments of the time of exposure to ultrasonic irradiation [37].

3.4. Effect of AO dye concentration on damage of BSA

The effect of different AO dye concentrations on the damage of BSA molecules was investigated by UV–vis and fluorescence spectra. The concentration of BSA was 1.0×10^{-5} mol/L, while the AO dye concentrations were changed from 0 to 2.5×10^{-5} mol/L at 0.5×10^{-5} mol/L interval.

It can be seen in Fig. 10(a) that the absorption peaks of BSA solution increase along with the increase of AO dye concentration whether with or without ultrasonic irradiation. However, the hyperchromic effects under ultrasonic irradiation increase more rapidly than the corresponding examples without ultrasonic irradiation only kept in dark. The changes of fluorescence spectra of the same BSA–AO solution were also reviewed. As can be seen from Fig. 10(b), whether with or without ultrasonic irradiation the fluorescence intensities of BSA solutions decrease along with the increase of AO dye concentration, which indicates that the fluorescence of BSA is quenched to a greater extent. Obviously, after being irradiated by ultrasound, the fluorescence intensity of BSA decreases much faster compared with that without ultrasonic irradiation kept in dark.

It can be inferred that, along with the increase of AO dye concentration, the quantity of $^1O_2$ generated in the solutions also increased gradually in unit time. The oxidation possibilities of $^1O_2$ to BSA molecules also become higher. The results demonstrate that AO dye as a sonosensitiser plays a very important role for the damage of BSA molecules in the BSA–AO solution. It can be seen that the anticipated level of protein damage can be also achieved by appropriately adjusting AO dye concentration.

3.5. Effect of solution acidity on damage of BSA

It is known that the pH value of microenvironment around the cancer tissue is slightly lower than that of the normal tissue. Therefore, we chose solution acidity as an influencing factor to review the damage of BSA. Here the pH values were adjusted from 5.0 to 9.0 using diluted HCl and Tris solutions. The concentrations of BSA and AO dye were both 1.0×10^{-5} mol/L.

Fig. 11(a) shows the absorption peaks of BSA–AO solutions at 278 nm either with or without ultrasonic irradiation both decrease along with the increase of pH value. Certainly, the absorption peaks

of BSA–AO solution under ultrasonic irradiation express more obvious hyperchromic effect compared with those without ultrasonic irradiation kept in dark. Correspondingly, Fig. 11(b) shows the fluorescence intensities of BSA–AO solution enhanced along with the increase of pH value. The fluorescence intensities are much low after being irradiated by ultrasound compared with those kept in dark.

The results indicate that the BSA molecules are difficult to damage in the range of high pH values. It is well known that the isoelectric point (p*I*) of BSA in aqueous solution is about pH = 4.8. When the solution pH value is higher than p*I*, the surface of BSA molecules bears negative charges. Contrarily, when the solution pH value is lower than p*I*, the surface bears positive charges. In this experiment, in order to review the influence of solution acidity on the damage of BSA, the pH value was set from 5.0 to 9.0 thus in the BSA–AO solution the BSA should possess a negative charge. At the same time, as a chloride, AO dye exists as cationic form in a comparably wide range of pH value ($8.0 > pH > 3.0$). Even in weak acidic solution ($7.0 > pH > 4.8$), because the BSA bears some negative charges, the AO dye cation is close to it. Hence, the interaction between BSA and AO dye occurs easily. However, in alkali condition, the hydrogen ions of AO dye are neutralized. Thus, the electrostatic interaction becomes weak. The electrostatic interaction is a part of the binding force between the BSA and AO dye. Due to the decrease of interaction force or the increase of repulsion between both, the possibility of damaging BSA decreases along with the increase of pH value. From the experiment, it is showed that the damage of protein is easier in weak acidity, which is advantage to the tumor treatment.

3.6. Effect of ionic strength on damage of BSA

In order to determine the effect of the ionic strength on sonodynamic damage of BSA, some related experiments were carried out using different concentrations of NaCl salt from 0 to 200 mmol/L at 50 mmol/L interval. The concentrations of BSA and AO were both 1.0×10^{-5} mol/L.

Fig. 12(a) shows that the absorption peak of BSA–AO solution at 278 nm either with or without ultrasonic irradiation increases along with the increase of solution ionic strength. Of course, under ultrasonic irradiation, they become much higher compared to those without ultrasonic irradiation. Fig. 12(b) shows that the fluorescence intensity of BSA–AO solution decreases along with the increase of ionic strength. Obviously, because of the oxidative damage of Trp and Tyr residues, the fluorescence intensity is lower than that without ultrasonic irradiation maintained in the dark.

The results indicate that the BSA molecules in BSA–AO solution under ultrasonic irradiation are damaged more seriously along with the increase of ionic strength. In this process, the increase of the ionic strength causes the salt bonds in BSA molecules to be ruptured, which results in the breakdown of the secondary structure, extension of peptide strand and exposure of Trp, Tyr and Phe residues. Moreover, along with the increase of the ionic strength, the accessibility of AO dye to chromophoric amino acid residues of BSA becomes easier. Therefore, the oxidative damage degree of BSA increases along with the increase of the ionic strength.

3.7. Possible mechanism of sonodynamic damage of BSA in the presence of AO dye under ultrasonic irradiation

The method utilizing ultrasonic irradiation combining with sonosensitisers (such as some photosensitive dyes) to restrain and kill cancer cells was firstly called sonodynamic therapy (SDT) by Umenmura S. Because of the selectivity and collectivity of sonosensitisers to cancer cells and the low power ultrasonic irradiation, the SDT attracted researchers' attention. However, until now, there has been no established mechanism and satisfactory explanation on the damage of BSA under ultrasonic irradiation in the presence of sonosensitisers. Usually, the following two points of view, namely, "sonoluminescence" and "high-heat excitation" may be accepted to explain the damage process. Firstly, it is well known that the sonoluminescence caused by ultrasonic cavitation generates light of broad wavelength. This light can excite the AO dye to act as a photosensitiser. In fact, this is the damage mechanism of PDT [38]. Secondly, it is well known that the temperature produced by ultrasonic cavitation in water medium can generally reach 10^5 °C and 10^6 °C, so high temperature sufficiently can excite the sonosensitisers [39]. Both light and heat energies can activate AO dye. Their excited state can transfer the energy to triplet oxygen ($^3O_2$) in solution, producing $^1O_2$ with high oxidation activity. The above experimental results reveal that AO dye can interact with BSA molecules through electrostatic and hydrophobic forces, which enable the AO dye to oxidize BSA molecules easily in a short time. It is known that both heat and light energies come from ultrasonic cavitation. However, it needs further research to validate which kind of energy the AO dye makes use of. In this study, AO dye was adopted as a sonosensitiser to damage BSA molecules under ultrasonic irradiation. The results suggest that the AO dye molecules have a high oxidative activity during the sonodynamic damage process.

4. Conclusion

In this paper, the interaction of BSA and AO and the damage of BSA in the presence of AO under ultrasonic irradiation were investigated by UV–vis and fluorescence spectra. The experimental results show that AO molecules can bind to BSA molecules with high affinity, and quench the intrinsic fluorescence of BSA efficiently. According to fluorescence quenching calculation, the static quenching mechanism, the binding constant ($K_A = 2.01 \times 10^4$ L/mol) and the binding site number ($n = 1.00$), binding distance ($r = 3.21$ nm) were obtained. In addition, it had been detected that the damage of BSA happened under low frequency (59 kHz) ultrasonic irradiation in the presence of AO dye determined by UV–vis and fluorescence spectra. Meanwhile, the influences of ultrasonic irradiation time, AO dye concentration, ionic strength and solution acidity on the damage of BSA were also studied. The results show that the degree of damage to BSA molecules increases with the increase of ultrasonic irradiation time and AO dye concentration. Nevertheless, it slightly decreases with the pH values and increases with the ionic strength. Hence, it can be inferred that the synergetic effect of ultrasonic irradiation and AO dye can easily damage the BSA molecules.

Acknowledgments

The authors greatly acknowledge the National Natural Science Foundation of China for financial support. The authors also thank our colleagues and other students for their participating in this work.

References

[1] Lu CS, Mai FD, Wu CW, Wu RJ, Chen CC. Titanium dioxide-mediated photocatalytic degradation of Acridine Orange in aqueous suspensions under UV irradiation. Dyes Pigments 2008;76:706–13.
[2] Lauretti F, Lucas de Melo F, Benati FJ, de Mello Volotao E, Santos N, Linhares RE, et al. Use of acridine orange staining for the detection of rotavirus RNA in polyacrylamide gels. J Virol Methods 2003;114:29–35.
[3] Cao Y, He XW, Gao Z, Peng L. Fluorescence energy transfer between Acridine Orange and Safranine T and its application in the determination of DNA. Talanta 1999;49:377–83.

[4] Bi SY, Qiao CY, Song DQ, Tian Y, Gao DJ, Sun Y, et al. Study of interactions of flavonoids with DNA using acridine orange as a fluorescence probe. Sensor Actuat B 2006;19:199–208.
[5] Murza A, Sanchez-Cortes S, Garcia-Ramos JV, Guisan JM, Alfonso C, Rivas G. Interaction of the antitumor drug 9-aminoacridine with guanidinobenzoatase studied by spectroscopic methods: a possible tumor marker probe based on the fluorescence exciplex emission. Biochemistry 2000;39:10557–65.
[6] Usacheva MN, Teichert MC, Biel MA. The role of the methylene blue and toluidine blue monomers and dimers in the photoinactivation of bacteria. J Photochem Photobiol B 2003;71:87–98.
[7] Fisher AMR, Murphree AL, Gomer CJ. Clinical and preclinical photodynamic therapy. Laser Surg Med 1995;17:2–31.
[8] Carter DC, Ho JX. Structure of serum albumin. Adv Protein Chem 1994;45:153–203.
[9] Zsila F, Bikadi Z, Simonyi M. Probing the binding of the flavonoid, quercetin to human serum albumin by circular dichroism, electronic absorption spectroscopy and molecular modelling methods. Biochem Pharmacol 2003;65:447–56.
[10] Olson RE, Christ DD. Plasma protein binding of drugs. Annu Rep Med Chem 1996;31:327–37.
[11] Dockal M, Carter DC, Ruker F. Conformational transitions of the three recombinant domains of human serum albumin depending on pH. J Biol Chem 2000;275:3042–50.
[12] Dougherty TJ, Kaufman JE, Goldfarb A. Photoradiation therapy for the treatment of malignant tumors. Cancer Res 1978;38:2628–35.
[13] Dougherty TJ, Lawrence G, Kaufman JE, Boyle DG, Weishaupt KR, Goldfarb A. Photoradiation in the treatment of recurrent breast carcinoma. J Natl Cancer Inst 1979;62:231–7.
[14] Doughtery TJ, Grindery GB, Fiel R, Weishaupt KR, Boyle DG. Photoradiation therapy. II. Cure of animal tumors with hematoporphyrin and light. J Natl Cancer Inst 1975;55:115–21.
[15] Umemura S, Yumita N, Nishigaki R. Enhancement of ultrasonically induced cell damage by a gallium–porphyrin complex, ATX-70. Jpn J Cancer Res 1993;84:582–8.
[16] Wilkinson F, Helman WP, Ross AB. Rate constants for the decay and reactions of the lowest electronically excited singlet state of molecular oxygen in solution. J Phys Chem Ref Data 1995;24:663–1021.
[17] Davies MJ. Singlet oxygen-mediated damage to proteins and its consequences. Biochem Biophys Res Commun 2003;305:761–70.
[18] Epe B, Pflaum M, Boiteux S. DNA damage induced by photosensitizers in cellular and cell-free systems. Mutat Res 1993;299:135–45.
[19] Tachibana K, Kimura N, Okumura M, Eguchi H, Tachibana S. Enhancement of cell killing of HL-60 cells by ultrasound in the presence of the photosensitizing drug Photofrin II. Cancer Lett 1993;72:195–9.
[20] Yumita N, Nishigaki R, Umemura K. Synergistic effect of ultrasound and hematoporphyrin on Sarcoma 180. Jpn J Cancer Res 1990;81:304–8.
[21] Yumita N, Nishigaki R, Umemura K. Hematoporphyrin as sensitizer of cell damaging effect of ultrasound. Jpn J Cancer Res 1989;80:219–22.
[22] Umemura S, Yumita N, Nishigaki R. Mechanism of cell damage by ultrasound in combination with hematoporphyrin. Jpn J Cancer Res 1990;81:962–6.
[23] Suzuki T, Kamada S, Yoshida Y, Unno K. A study of sonodynamic therapy–antitumor effect on novel sonodynamic compounds under ultrasound. Heterocycles 1994;38:1209–11.
[24] Umemura S, Yumita N, Umemura K, Nishiigaki R. Sonodynamically induced effect of rose bengal on isolated sarcoma 180 cells. Cancer Chemother Pharmacol 1999;43:389–93.
[25] Moan J, Berg K. The photodegradation of porphyrins in cells can be used to estimate the lifetime of singlet oxygen. Photochem Photobiol 1991;53:549–53.
[26] Feng XZ, Lin Z, Yang LJ, Wang C, Bai C. Investigation of the interaction between acridine orange and bovine serum albumin. Talanta 1998;47:1223–9.
[27] Kang J, Liu Y, Xie M, Li S, Jiang M, Wang Y. Interactions of human serum albumin with chlorogenic acid and ferulic acid. Biochim Biophys Acta 2004;1674:205–14.
[28] Wang CX, Yan FF, Zhang YX, Ye L. Spectroscopic investigation of the interaction between rifabutin and bovine serum albumin. J Photochem Photobiol A 2007;192:23–8.
[29] Shang L, Jiang X, Dong SJ. In vitro study on the binding of neutral red to bovine serum albumin by molecular spectroscopy. J Photochem Photobiol A 2006;184:93–7.
[30] Krieglstein J, Meiler W, Staab J. Hydrophobic and ionic interactions of phenothiazine derivatives with bovine serum albumin. Biochem Pharmacol 1972;21:985–97.
[31] Sklar LA, Hudson BS, Simoni RD. Conjugate polyene fatty acids as fluorescent membrane probes. Biochemistry 1977;16:5100–8.
[32] Wang YP, Wei YL, Dong C. Study on the interaction of 3,3-bis(4-hydroxy-1-naphthyl)-phthalide with bovine serum albumin by fluorescence spectroscopy. J Photochem Photobiol A 2006;177:6–11.
[33] Yumita N, Nishigaki R, Umemura K, Morse PD, Swartz HM, Cain CA, et al. Sonochemical activation of hematoporphyrin: an ESR study. Radiat Res 1994;138:171–6.
[34] Hu YJ, Liu Y, Zhao RM, Dong JX, Qu SS. Spectroscopic studies on the interaction between methylene blue and bovine serum albumin. J Photochem Photobiol A 2006;179:324–9.
[35] Finley EL, Dillon J, Crouch RK, Schey KL. Identification of tryptophan oxidation products in bovine a-crystallin. Protein Sci 1998;7:2391–7.
[36] Mantulin WW, Rohde MF, Gotto AM, Pownall HJ. The conformational properties of human plasma apolipoprotein C-II. J Biol Chem 1980;255:8185–91.
[37] Biplab B, Alok D. Interaction of Chlorin p6 with bovine serum albumin and photodynamic oxidation of protein. J Photochem Photobiol B 2006;85:49–55.
[38] Miyoshi N, Igarashi T, Riesz P. Evidence against singlet oxygen formation by sonolysis of aqueous oxygen-saturated solutions of hematoporphyrin and rose bengal: the mechanism of sonodynamic therapy. Ultrason Sonochem 2000;7:121–4.
[39] Miyoshi N, Tuziuti T, Yasui K, Iida Y, Shimizu N, Riesz P, et al. Ultrasound-induced cytolysis of cancer cells is enhanced in the presence of micron-sized alumina particles. Ultrason Sonochem 2008;15:881–90.